Prognostic value of apparent diffusion coefficient in neuroendocrine carcinomas of the uterine cervix

Jian Chen [1], **Ning Ma** [2], **Mingyao Sun** [3], **Li Chen** [1], **Qimin Yao** [4], **XingFa Chen** [2], **Cuibo Lin** [1], **YongWei Lu** [1], **Yingtao Lin** [5], **Liang Lin** [1], **XueXiong Fan** [6], **Yiyu Chen** [7], **Jingjing Wu** [1], **Haixin He** [Corresp. 1]

[1] Department of Gynecology, Clinical Oncology School of Fujian Medical University, Fujian Cancer Hospital, Fuzhou, Fujian, China

[2] Department of Radiology, Clinical Oncology School of Fujian Medical University, Fujian Cancer Hospital, Fuzhou, Fujian, China

[3] Department of Clinical Nutrition, Fujian Provincial Hospital, Fuzhou, Fujian, China

[4] College of Finance, Fujian Jiangxia University, Fuzhou, Fujian, China

[5] Department of Drug Clinical Trial Institution, Clinical Oncology School of Fujian Medical University, Fujian Cancer Hospital, Fuzhou, Fujian, China

[6] Department of Medical Record, Clinical Oncology School of Fujian Medical University, Fujian Cancer Hospital, Fuzhou, Fujian, China

[7] Department of Pathology, Clinical Oncology School of Fujian Medical University, Fujian Cancer Hospital, Fuzhou, Fujian, China

Corresponding Author: Haixin He
Email address: 63804657@qq.com

Objectives: This research was designed to examine the associations between the apparent diffusion coefficient (ADC) values and clinicopathological parameters, and to explore the prognostic value of ADC values in predicting the International Federation of Gynecology and Obstetrics (FIGO) stage and outcome of patients suffering from neuroendocrine carcinomas of the uterine cervix (NECCs).

Methods: This retrospective study included 83 patients with NECCs, who had undergone pre-treatment magnetic resonance imaging (MRI) between November 2002 and June 2019. The median follow-up period was 50.7 months. Regions of interest (ROIs) were drawn manually by two radiologists. ADC values in the lesions were calculated using the Functool software. These values were compared between different clinicopathological parameters groups. The Kaplan–Meier approach was adopted to forecast survival rates. Prognostic factors were decided by the Cox regression method.

Results: In the cohort of 83 patients, 9, 42, 23, and 9 patients were in stage I, II, III, and IV, respectively. ADC_{mean}, ADC_{max}, and ADC_{min} were greatly lower in stage IIB–IVB than in stage I–IIA tumours, as well as in tumours measuring $\geq$ 4 cm than in those < 4 cm. ADC_{mean}, FIGO stage, and age at dianosis were independent prognostic variables for the 5-year overall survival (OS). ADC_{min}, FIGO stage, age at diagnosis and para-aortic lymph node metastasis were independent prognostic variables for the 5-year progression-free survival (PFS) in multivariate analysis. For surgically treated patients (n=45), ADC_{max} was an independent prognostic parameter for both 5-year OS and 5-year PFS.

Conclusions: ADC_{mean}, ADC_{min}, and ADC_{max} are independent prognostic factors for NECCs. ADC analysis could be useful in predicting the survival outcomes in patients with NECCs.

1 **Prognostic value of Apparent Diffusion Coefficient in neuroendocrine**

2 **carcinomas of the uterine cervix.**

3 Jian Chen[1], Ning Ma[2], Mingyao Sun[3], Li Chen[1], Qimin Yao[4], XingFa Chen[2], CuiBo Lin[1],

4 YongWei Lu[1], Yingtao Lin[5], Liang Lin[1], XueXiong Fan[6], Yiyu Chen[7], Jingjing Wu[1], Haixin

5 He[1,*].

6 [1] Department of Gynecology, Clinical Oncology School of Fujian Medical University, Fujian

7 Cancer Hospital. Fuzhou, 350014, China

8 [2] Department of Radiology, Clinical Oncology School of Fujian Medical University, Fujian

9 Cancer Hospital. Fuzhou, 350014, China

10 [3] Department of Clinical Nutrition, Fujian Provincial Hospital, Fujian 350001, China

11 [4] College of Finance, Fujian Jiangxia University, Fujian 350001, China

12 [5] Department of Drug Clinical Trial Institution, Clinical Oncology School of Fujian Medical

13 University, Fujian Cancer Hospital. Fuzhou, 350014, China

14 [6] Department of Medical Record, Clinical Oncology School of Fujian Medical University, Fujian

15 Cancer Hospital. Fuzhou, 350014, China

16 [7] Department of Pathology, Clinical Oncology School of Fujian Medical University, Fujian

17 Cancer Hospital. Fuzhou, 350014, China

18 Corresponding Author:

19 Haixin He[1]

20 Department of Gynecology, Clinical Oncology School of Fujian Medical University, Fujian

21 Cancer Hospital. Fuzhou, 350014, China

22   Email address: 63804657@qq.com

23   **Abstract**

24   **Objectives:** This research was designed to examine the associations between the apparent

25   diffusion coefficient (ADC) values and clinicopathological parameters, and to explore the

26   prognostic value of ADC values in predicting the International Federation of Gynecology and

27   Obstetrics (FIGO) stage and outcome of patients suffering from neuroendocrine carcinomas of

28   the uterine cervix (NECCs).

29   **Methods**: This retrospective study included 83 patients with NECCs, who had undergone pre-

30   treatment magnetic resonance imaging (MRI) between November 2002 and June 2019. The

31   median follow-up period was 50.7 months. Regions of interest (ROIs) were drawn manually by

32   two radiologists. ADC values in the lesions were calculated using the Functool software. These

33   values were compared between different clinicopathological parameters groups. The Kaplan–

34   Meier approach was adopted to forecast survival rates. Prognostic factors were decided by the

35   Cox regression method.

36   **Results**: In the cohort of 83 patients, 9, 42, 23, and 9 patients were in stage I, II, III, and IV,

37   respectively. ADC_{mean}, ADC_{max}, and ADC_{min} were greatly lower in stage IIB–IVB than in stage

38   I–IIA tumours, as well as in tumours measuring $\geq$ 4 cm than in those < 4 cm. ADC_{mean}, FIGO

39   stage, and age at diagnosis were independent prognostic variables for the 5-year overall survival

40   (OS). ADC_{min}, FIGO stage, age at diagnosis and para-aortic lymph node metastasis were

41   independent prognostic variables for the 5-year progression-free survival (PFS) in multivariate

42   analysis. For surgically treated patients (n=45), ADC_{max} was an independent prognostic

43   parameter for both 5-year OS and 5-year PFS.

44   **Conclusions:** ADC_{mean}, ADC_{min}, and ADC_{max} are independent prognostic factors for NECCs.

45   ADC analysis could be useful in predicting the survival outcomes in patients with NECCs.

46   **Keywords:** Neuroendocrine carcinoma of the uterine cervix, Apparent diffusion coefficients,

47   Prognostic factors,   Diffusion-weighted imaging

Introduction

Neuroendocrine carcinomas of the cervix (NECCs), an infrequent but highly invasive form of cervical cancer, represent less than 5% of cervical carcinomas (Gardner et al. 2011; Li et al. 2020; Lin et al. 2020; Satoh et al. 2014). According to the World Health Organization classification, NECCs are divided into small cell neuroendocrine carcinomas (SCNECs) and large cell neuroendocrine carcinomas (LCNECs) (Satoh et al. 2014). Owe to the high incidence of early lymph node involvement and distant metastasis, the outcome of patients with NECCs is worse than those with other subtypes of cervical cancer. Radical surgery and chemoradiation are recommended as the primary treatment for patients with early- and advanced-stage disease, respectively (Bhatla et al. 2019). Due to the rarity of NECCs, most studies on NECCs are reported in small samples or are case reports (McCann et al. 2013; Yuan et al. 2015). Therefore, the prognostic parameters and treatment of NECCs are controversial. Advanced FIGO stage, lymph node involvement, large tumor size, older age and lymphovascular invasion have been reported to be associated with poor prognosis (Chen et al. 2021; Gadducci et al. 2017). However, the described factors play a limited role in predicting the prognosis of NECCs.

MRI is a great tool for diagnosing and staging cervical tumours due to its high soft tissue resolution. On T1- and T2-weighted images (T1WI and T2WI, respectively) as well as contrast-enhanced images, MRI can show both morphologic and signal intensity properties (Nakamura et al. 2012). Diffusion-weighted imaging (DWI), a functional imaging technology, quantifies the free movement of water molecules (Brownian molecular movement) through ADC values (Bruix & Llovet 2002; Fan et al. 2020). ADC describes the velocity and scope of molecular diffusion

69 movements in various directions (Liang et al. 2016). Moreover, ADC values provide useful

70 information about tumour aggressiveness, subtype characterisation, and treatment responses

71 taking into consideration the limiting barriers in tissue compartments (De Robertis et al. 2018;

72 Gu et al. 2019; Meyer et al. 2019; Perucho et al. 2020; Zou et al. 2019). Schob et al. found that

73 ADC value were useful in predicting lymphatic metastasis, and proliferative activity in thyroid

74 cancer (Schob et al. 2017a). In gastric cancer, Liu et al demonstrated that ADC analysis is

75 helpful to assess the pre-treatment T and N staging (Liu et al. 2014). To date, few studies have

76 discussed the application of MRI in NECCs. Duan et al. found that NECCs are characterized by

77 lower ADC values and homogeneous lesion texture on MRI images (Duan et al. 2016). However,

78 no studies have reported the utility of ADC values in predicting the outcomes of patients with

79 NECCs. In this study, we examined the associations between maximum, mean, and minimum

80 ADC values (ADC_{max}, ADC_{mean} and ADC_{min}, respectively) and clinicopathological parameters, as

81 well as the prognostic value of ADC values in predicting the stage and outcome in patients with

82 NECCs, in a retrospective review of 83 patients. We also assessed the accuracy of MRI in the

83 diagnosis of NECCs.

84 **Materials & Methods**

85 **Patients and treatment**

86 The research was approved by the Ethics Committee of Fujian Medical University Cancer

87 Hospital (Reference No: K2021-043-01). Between November 2002 and June 2019, the

88 clinicopathological information of 172 patients with pathological confirmed NECCs who

89 received treatment at Fujian Medical University Cancer Hospital, were reviewed. All histologic

90   slides were reviewed by two experienced pathologists to confirm the diagnosis of NECCs. The

91   requirement for informed consent was waived due to the retrospective nature of this study. The

92   following were the standards for inclusion: (1) those with pathological confirmed NECCs, (2)

93   those who underwent pre-treatment abdominal and pelvic MRI in our centre, and (3) those who

94   received treatment in our centre and had complete medical records. The exclusion standards were

95   as shown: (1) presence of other concurrent malignancies, (2) history of cancer, (3) those who

96   refused or discontinued treatment, and (4) lost to follow-up. Finally, 83 patients were recruited in

97   the group.

98   **MRI imaging**

99   A 1.5T MRI system (GE Signa HDxT) was used. Before the examination, the patients were

100   required to drink enough water to fill their bladder to a moderate level. The MRI scan extended

101   from the renal hilum to the perineum. Routine abdominal and pelvic MRI including the

102   following sequences were acquired as follows: (1) sagittal T2WI: fast spin-echo (FSE) sequence,

103   repetition time (TR) / echo time (TE), 4760/104 ms; matrix size, 320 × 192; field of view (FOV),

104   24 cm; slice thickness/intersection gap, 5/1 mm; (2) axial T2WI: TR/TE, 4320/105 ms; matrix

105   size, 320 × 192; FOV, 24 cm; slice thickness/intersection gap, 5/1 mm; (3) axial T1WI: fast FSE

106   sequence; TR/TE, 600/7.7 ms; matrix size, 320 × 256; FOV, 48 cm; slice thickness/intersection

107   gap, 7/1 mm. The protocols for axial DWI (b = 0, 800 s/mm^2) were as follows: TR, 4225 ms, TE,

108   minimum time; matrix size, 128 × 128; FOV, 38 cm; slice thickness/intersection gap, 7/1 mm.

109   **Imaging analysis**

110   All images were retrieved from the local picture archiving and communication systems. Two

111   radiologists analysed the MR images in consensus (N.M. and X.F.C, with 8 and 12 years of

112   experience in gynaecologic imaging, respectively). The two radiologists agreed on the criteria for

113   determining the tumour size, vaginal extension, parametrial extension, and lymph node

114   metastasis according to the FIGO 2018 staging and the guidance of the European Society of

115   Urogenital Radiology (Balleyguier et al. 2011; Bhatla et al. 2018). They were blinded to the

116   patients' information. The ADC map was constructed automatically using the Functool software

117   on the Advantage Workstation(AW 4.2 version, GE, US. https://www.medicalexpo.com/product-

118   manufacturer/ge-mri-system-15892-438.html). Regions of interest (ROIs) were manually drawn

119   along the margin of the lesions showing maximal tumour size on axial DWI images. The ROI

120   did not include parts of the tumour that were cystic, necrotic, or haemorrhagic. ADC values in

121   the lesions were calculated using the software (Fig. 1).

122   **Treatment**

123   Since this was a retrospective study, therefore, the treatment plans of most cases were largely

124   dependent on FIGO 2008 guidelines. Surgery was the primary treatment for patients in the early

125   stage (FIGO stage I–IIA), and chemoradiation was applied for patients in the advanced stage

126   (FIGO stage III–IV). For patients with IIB stage, whether to undergo surgery after neoadjuvant

127   therapy or received chemoradiation treatment depends on the doctor's judgment. According to

128   the postoperative pathology report, adjuvant therapy was performed if there were risk factors

129   such as lymph node metastases, positive margin, deep stromal invasion, lymphovascular invasion,

130   parametrial invasion, and perineural invasion. Finally, 45 patients received surgery and 38

131 patients received chemoradiation or only chemotherapy. Of the 80 patients who received

132 chemotherapy, 38 received etoposide and cisplatin/carboplatin (EP regimen), and 34 received

133 paclitaxel and cisplatin/carboplatin (TP regimen). The other eight patients received

134 bleomycin, ifosfamide, and cisplatin (one case); paclitaxel, etoposide, and cisplatin (three cases);

135 docetaxel and platinum (two cases); and TP and EP successively (two cases).

136 **Statistical analysis**

137 ADC values are shown as mean ± SD. The normality of all the data was tested by applying the

138 Kolmogorov–Smirnov test. The Student's t-test or the Mann–Whitney U test was adopted to

139 compare the ADC values among different tumour groups. Applying the maximum Youden's

140 index, the ROC curve was used to estimate the parameter cutoff values. The Kaplan–Meier and

141 Cox regression methods were adopted to calculate prognostic factors for OS and PFS. The

142 multivariate analysis further investigated prognostic parameters (p values <0.1) from the

143 univariate analysis. P value <0.05 was regarded statistically significant. The SPSS version 24.0

144 statistical software (SPSS Inc. Chicago, IL, USA, http://www.spss.com) was employed to

145 perform all statistical analyses.

146 **Results**

147 **Clinicopathologic characteristics of the patients**

148 The clinicopathological characteristics of the patients are listed in Table 1. Eighty-three

149 patients were enrolled; their ages ranged from 25 to 78 years, and the average age was 49.2 years.

150 The average size of the cervical tumour was 4.7 cm. On the basis of the FIGO 2018 staging

151 system, 9, 42, 23, and 9 patients were in stage I, II, III, and IV, respectively. There were 80 and 3

152 cases of SCNEC and LCNEC, respectively. Pure histology was documented in 68.7% (57/83) of

153 the patients. The mixed histology patterns included adenocarcinoma (16/83 patients; 19.3%),

154 squamous cell carcinoma (7/83 patients; 8.4%), and adenosquamous carcinoma (3/83 patients;

155 3.6%). In the cohort of 83 patients, the mean values of ADC_{max}, ADC_{mean}, and ADC_{min} were

156 0.969, 0.750 and 0.632 ($\times 10^{-3}$ mm^2/s), respectively.

157 **Associations between ADC values and clinicopathological parameters**

158 The results of the Mann–Whitney U test and Student's t-test for the comparison between ADC

159 values and clinicopathological features are presented in Table 2. The ADC_{mean} of the primary

160 tumour had a high correlation with the FIGO stage (I-IIA vs. IIB-IVB, 0.880 ± 0.327 vs. 0.655 ±

161 0.226, p=0.001), tumour size (<4cm vs. >4cm, 0.882 ± 0.305 vs. 0.696 ± 0.274, p=0.002), pelvic

162 lymph node metastasis (negative vs positive, 0.788 ± 0.332 vs. 0.672 ± 0.172, p=0.04), and depth

163 of stromal invasion (inner third vs middle to outer third, 0.975 ± 0.378 vs. 0.748 ± 0.264,

164 p=0.04). The ADC_{max} of the pre-treatment tumour was greatly related to tumour size (<4cm vs.

165 >4cm, 1.069 ± 0.269 vs. 0.928 ± 0.282, p=0.022), FIGO stage (I-IIA vs. IIB-IVB, 1.068 ± 0.299

166 vs. 0.896 ± 0.252, p=0.01), and depth of stromal invasion (inner third vs middle to outer third,

167 1.162 ± 0.352 vs. 0.951 ± 0.264, p=0.023). The ADC_{min} was significantly associated with

168 tumour size (<4cm vs. >4cm, 0.751 ± 0.335 vs. 0.583 ± 0.262, p=0.007), FIGO stage (I-IIA vs.

169 IIB-IVB, 0.761 ± 0.345 vs. 0.538 ± 0.206, p=0.001), and pelvic lymph node metastasis (negative

170 vs positive, 0.678 ± 0.329 vs. 0.534 ± 0.165, p=0.009).

171 **MRI and pathological staging of NECCs**

172   Among the 45 patients who receiving surgery, 30 patients receiving neoadjuvant therapy were

173   excluded, and finally, 15 patients were included in the analysis to calculate the MRI accuracy.

174   Table 3 shows the agreement between the MRI stage and the pathological stage. The overall

175   accuracy of MRI was only 46% (7/15). Errors were seen in eight patients due to false-negative

176   (n=2) or false-positive (n=3) vaginal invasion, false-negative lymph node metastasis (n=1), or

177   false-positive parametrial invasion (n=2). The accuracy rates of MRI in the diagnosis of uterine

178   corpus invasion, parametrial invasion, vaginal invasion, and lymph node metastasis were 86.7%,

179   80.0%, 53.3%, and 93.3%, respectively.

180   **Survival results**

181   The median OS and PFS of the enrolled 83 patients were 42.7 and 38.1 months, and the 5-year

182   OS and PFS rates were 46.3 and 41.4%, respectively. The median follow-up period for all

183   patients was 50.7 months (range: 2–193 months). At the end of follow-up period, cancer

184   recurrence was observed in 47 patients, 41 patients had died. Patients with stage I, II, III, and IV

185   disease had 5-year OS rates of 88.9, 54.6, 35.5, and 0%, respectively. Patients with stage I, II, III,

186   and IV disease had 5-year PFS rates of 77.8, 53.9, 21.9, and 0%, respectively. ROC curve

187   analyses were performed to decide whether ADC values predicted the prognosis of patients

188   diagnosed with NECCs. The optimal ADC_{mean}, ADC_{max}, and ADC_{min} cutoff values for OS were

189   0.701×10^{-3} mm^2/s, 1.041×10^{-3} mm^2/s, and 0.822×10^{-3} mm^2/s (AUC: 0.680, 0.717 and 0.614),

190   respectively. The optimal ADC_{mean}, ADC_{max}, and ADC_{min} cutoff values for PFS were 0.969×10^{-3}

191   mm^2/ss, 0.997×10^{-3} mm^2/ss, and 0.922×10^{-3} mm^2/s(AUC: 0.664, 0.696, and 0.633),

192   respectively (Fig. 2).

Prognostic factors

194   Multivariate analyses showed that ADC_{mean} ($\leq 0.7 \times 10^{-3}$ mm^2/s vs. >0.7 $\times 10^{-3}$ mm^2/s,

195   HR=2.344, 95% CI=[1.155,4.756], p=0.018), advanced FIGO stage (HR=2.085, 95%

196   CI=[1.351,3.217], p=0.001), and age (> 45 vs. $\leq$ 45 years, HR=2.651, 95% CI=[1.257,5.590],

197   p=0.01) were independent prognostic factors for OS. Besides, ADC_{min} ($\leq 0.68 \times 10^{-3}$ mm^2/s vs. >

198   0.68×10^{-3} mm^2/s, HR=3.787, 95% CI=[1.469,9.765], p=0.006), FIGO stage (HR=1.919, 95%

199   CI=[1.221,3.014], p=0.005), age (> 45 vs. $\leq$ 45 years, HR=2.380, 95% CI=[1.222,4.635],

200   p=0.011) , and para-aortic lymph node metastasis (positive vs negative, HR=3.151, 95%

201   CI=[1.204,8.248], p=0.019) were significant prognostic parameters for PFS (Table 4). Survival

202   curves for patients with various ADC values, FIGO stage, ages, and para-aortic lymph node

203   statuses were shown in the Figure 3 and Figure 4. In patients who received surgery, patients with

204   ADC_{max} >1.032 $\times 10^{-3}$ mm^2/s had significantly better 5-year OS (92.9% vs. 36.9%, p=0.006) and

205   5-year PFS (83.7% vs. 30.0%, p=0.006) rates than those with $ADC_{max} \leq 1.032 \times 10^{-3}$ mm^2/s.

206   Besides, lymphovascular invasion was another prognostic factor that affected OS (negative vs.

207   positive: 76.1% vs. 38.3%; p=0.009) (Table 5).

Discussion

209   To the best of our knowledge, this study was the first to investigate the prognostic utility of

210   ADC values in predicting the outcomes of patients with NECCs. Moreover, the correlation

211   between the ADC values and clinicopathological parameters in neuroendocrine carcinomas has

212   been reported for the first time. We also assessed the accuracy of MRI in the diagnosis of

213   NECCs. It was previously suggested that the decreased ADC values in malignant tumours

214   indicated proliferative activity and increased tissue cellularity, which led to the disordered

215   arrangement of the intracellular structure and decreased extracellular spaces (Nakamura et al.

216   2012; Schob et al. 2017b). Additionally, some studies have reported that ADC values reflect the

217   tumour aggressiveness and predicted prognosis and treatment response to chemoradiation

218   therapy. Robertis et al. found that ADC maps may help predict the tumour grade, vascular

219   involvement, and nodal and liver metastases in pancreatic neuroendocrine tumours (De Robertis

220   et al. 2018). Heo et al. showed that pre-treatment ADC values could predict the tumour

221   recurrence in patients who were diagnosed with cervical cancer and treated with chemoradiation

222   (Heo et al. 2013). They found that patients with the 75th percentile ADC > 0.936×10^{-3} mm^2/s

223   had significantly better overall recurrence free survival raterates than those with the 75th

224   percentile ADC $\leqslant 0.936 \times 10^{-3}$ mm^2/s (91.7% vs. 51.9%, p=0.003) . Other researches have also

225   shown that ADC analysis may be an effective clinical biomarker to forecast treatment response

226   and survival rate among patients with hepatocellular carcinoma and rectal cancer (Choi et al.

227   2016; Shaghaghi et al. 2020). However, the efficacy of ADC values in predicting FIGO staging

228   and prognosis in patients with NECCs is unclear.

229   Therefore, we explored whether pre-treatment ADC values were associated with

230   clinicopathological characteristics in patients with NECC in this study. It was observed that

231   lower ADC values were greatly associated with advanced FIGO stage, large tumour size, deep

232   stromal invasion, and pelvic lymph node metastasis. We used the pre-treatment MRI and

233   demonstrated that ADC values were greatly related to the prognosis in patients with NECCs. In

234   multivariate analysis, ADC$_{mean}$ $\leqslant 0.7 \times 10^{-3}$ mm^2/s were associated with wores overall survival

235   rates (HR=2.344, p=0.018) and $ADC_{min} \leqslant 0.68 \times 10^{-3}$ mm^2/s were associated with worse

236   progression-free survival rates (HR=3.787, p=0.006). These findings are similar to those of a

237   prior study. Zhao et al. reported that pre-treatment ADC_{min} was significantly correlated with the

238   disease-free survival in patients with cervical cancer (HR=0.110, p=0.006) (Zhao et al. 2019). In

239   surgically treated patients, we found that $ADC_{max} \leqslant 1.032 \times 10^{-3}$ mm^2/s was greatly associated

240   with worse OS and PFS. The risk of recurrence and disease progression increased by 14.4 and

241   5.7 times, respectively, compared with those with $ADC_{max} > 1.032 \times 10^{-3}$ mm^2/s. ROC curve

242   analyses were performed to decide which ADC value among these three values performing the

243   best ability. ADC_{max} seems to have better diagnostic effectiveness than ADC_{mean} and ADC_{min},

244   and the AUC of ADC_{max} for OS and PFS was 0.717 and 0.696, respectively.

245   This research showed that FIGO stage and age at diagnosis were prognostic factors for OS,

246   and FIGO stage, age at diagnosis, and para-aortic lymph node metastasis were prognostic

247   parameters for PFS; these results are similar to those of our previous study (Chen et al. 2021).

248   Additionally, the lymphovascular invasion was founded to be a prognostic parameter for 5-year

249   OS in the patients who underwent surgery; however, FIGO stage was not. This may be due to the

250   fact that the proportion of lymphovascular invasion in patients with stage I disease (50.0%) was

251   higher than that in patients with stage II disease (32.1%).

252   MRI is regarded as a useful and accurate method for the diagnosis of cervical tumours. Sala et

253   al. found that MRI was 83% (8/41) accurate in diagnosing cervical carcinomas with vaginal

254   invasion (Sala et al. 2007). They assumed that this inaccuracy was caused by a large exophytic

255   cervical tumour stretching the vaginal fornix. A meta-analysis of 57 studies showed that the

256   sensitivity for parametrial invasion in MRI was 74% (Bipat et al. 2003). In our study, the

257   accuracy rates of MRI in the diagnosis of uterine corpus invasion, parametrial invasion, vaginal

258   invasion, and lymph node metastasis were 86.7%, 80.0%, 53.3%, and 93.3%, respectively. There

259   were two false-positive parametrial invasions. Cervical biopsy or cervical conisation was

260   performed before MRI examination, resulting in inflammation and stromal oedema; this resulted

261   in an inadequate estimation of parametrial invasion. Stromal oedema caused by tumour

262   compression is also a possible cause (Nakamura et al. 2012; Park et al. 2014). Additionally, Woo

263   et al. found that for determining parametrial invasion, oblique axial T2WI may be more accurate

264   than true axial T2WI, especially for tumours larger than 2.5 cm (Woo et al. 2019).

265   According to a meta-analysis of 72 studies comprising 5042 patients, MRI exhibited a

266   sensitivity of 56% and a specificity of 93% for detecting lymphadenopathy (Choi et al. 2010).

267   For detecting lymph node metastasis, the size criterion used in MRI was a short axis diameter ≥ 1

268   cm (Balleyguier et al. 2011; Dappa et al. 2017). This criterion, however, is flawed because it

269   overlaps with normal, hyperplastic, and metastatic lymph nodes. Furthermore, micrometastases

270   in negative lymph nodes are not rare (Lee et al. 2020). Therefore, we considered round shape,

271   irregular border, and necrosis as other signs of malignancy (Balleyguier et al. 2011). In our study,

272   the sensitivity, specificity and accuracy of MRI in detecting lymph node metastasis were 50.0%,

273   100%, and 93.3%, respectively. Lin et al. observed that the method combining tumour size and

274   ADC values had better sensitivity (25% vs. 83%) and similar specificity (98% vs. 99%)

275   compared with those of the traditional MRI approach (Lin et al. 2008). MRI was useful in

276 detecting the parametrial invasion, uterine corpus invasion, and lymph node metastasis; however,

277 the diagnostic efficacy of vaginal invasion needs to be improved.

278   There are several limitations in this research. First, this was a retrospective study; therefore,

279 selection bias was unavoidable. Second, we did not measure ADC values for the entire tumour in

280 this study. Further studies using histogram analyses will be needed. Moreover, ROIs were drawn

281 manually by two radiologists, and measurement errors were inevitable. Third, the study did not

282 include dynamic contrast-enhanced MRI, which is a useful diagnostic tool. Fourth, para-aortic

283 lymph node metastasis affected OS in our research as an independent prognostic parameter;

284 however; only 22% (10/45) of the patients had para-aortic lymph node dissection. Finally, this

285 was a single-centre study with a small sample size, especially for those with LCNECs. More

286 studies involving larger cohorts is needed.

287 **Conclusion**

288   It was observed that lower ADC values were greatly associated with advanced FIGO stage,

289 large tumour size, deep stromal invasion, and lymph node metastasis. ADC_{mean} and ADC_{min} were

290 independent prognostic parameters for NECCs. For surgically treated patients (n=45), ADC_{max}

291 was an independent prognostic parameter for both 5-year OS and PFS. Additionally, we found

292 that MRI is reliable for the prediction of uterine corpus invasion, parametrial invasion, and

293 lymph node metastasis, but not vaginal invasion. ADC analysis may be a useful tool for

294 predicting the FIGO stage and outcome of patients with NECCs.

295

296 **Acknowledgements**

297   We thank Xiaojie Wang for the helpful suggestions and comments on the manuscript. This work

298   was supported by the Fujian Medical University, funded by the Startup Fund for scientific

299   research (Grant number: 2020QH1216). The funders had no role in the study design, data

300   collection and analysis, decision to publish, or preparation of the manuscript.

301

References

302 **References**

303 Balleyguier C, Sala E, Da Cunha T, Bergman A, Brkljacic B, Danza F, Forstner R, Hamm B, Kubik-Huch R, Lopez C,
304 Manfredi R, McHugo J, Oleaga L, Togashi K, and Kinkel K. 2011. Staging of uterine cervical cancer with MRI:
305 guidelines of the European Society of Urogenital Radiology. *Eur Radiol* 21:1102-1110. 10.1007/s00330-
306 010-1998-x

307 Bhatla N, Aoki D, Sharma DN, and Sankaranarayanan R. 2018. Cancer of the cervix uteri. *Int J Gynaecol Obstet* 143
308 Suppl 2:22-36. 10.1002/ijgo.12611

309 Bhatla N, Berek JS, Cuello Fredes M, Denny LA, Grenman S, Karunaratne K, Kehoe ST, Konishi I, Olawaiye AB, Prat J,
310 Sankaranarayanan R, Brierley J, Mutch D, Querleu D, Cibula D, Quinn M, Botha H, Sigurd L, Rice L, Ryu HS,
311 Ngan H, Maenpaa J, Andrijono A, Purwoto G, Maheshwari A, Bafna UD, Plante M, and Natarajan J. 2019.
312 Revised FIGO staging for carcinoma of the cervix uteri. *Int J Gynaecol Obstet* 145:129-135.
313 10.1002/ijgo.12749

314 Bipat S, Glas AS, van der Velden J, Zwinderman AH, Bossuyt PM, and Stoker J. 2003. Computed tomography and
315 magnetic resonance imaging in staging of uterine cervical carcinoma: a systematic review. *Gynecol Oncol*
316 91:59-66. 10.1016/s0090-8258(03)00409-8

317 Bruix J, and Llovet JM. 2002. Prognostic prediction and treatment strategy in hepatocellular carcinoma. *Hepatology*
318 35:519-524. 10.1053/jhep.2002.32089

319 Chen J, Sun Y, Chen L, Zang L, Lin C, Lu Y, Lin L, Lin A, Dan H, Chen Y, and He H. 2021. Prognostic factors and
320 treatment of neuroendocrine tumors of the uterine cervix based on the FIGO 2018 staging system: a
321 single-institution study of 172 patients. *PeerJ* 9:e11563. 10.7717/peerj.11563

322 Choi HJ, Ju W, Myung SK, and Kim Y. 2010. Diagnostic performance of computer tomography, magnetic resonance
323 imaging, and positron emission tomography or positron emission tomography/computer tomography for
324 detection of metastatic lymph nodes in patients with cervical cancer: meta-analysis. *Cancer Sci* 101:1471-
325 1479. 10.1111/j.1349-7006.2010.01532.x

326 Choi MH, Oh SN, Rha SE, Choi JI, Lee SH, Jang HS, Kim JG, Grimm R, and Son Y. 2016. Diffusion-weighted imaging:
327 Apparent diffusion coefficient histogram analysis for detecting pathologic complete response to
328 chemoradiotherapy in locally advanced rectal cancer. *J Magn Reson Imaging* 44:212-220.
329 10.1002/jmri.25117

330 Dappa E, Elger T, Hasenburg A, Duber C, Battista MJ, and Hotker AM. 2017. The value of advanced MRI techniques
331 in the assessment of cervical cancer: a review. *Insights Imaging* 8:471-481. 10.1007/s13244-017-0567-0

332 De Robertis R, Maris B, Cardobi N, Tinazzi Martini P, Gobbo S, Capelli P, Ortolani S, Cingarlini S, Paiella S, Landoni L,
333 Butturini G, Regi P, Scarpa A, Tortora G, and D'Onofrio M. 2018. Can histogram analysis of MR images
334 predict aggressiveness in pancreatic neuroendocrine tumors? *Eur Radiol* 28:2582-2591. 10.1007/s00330-
335 017-5236-7

336 Duan X, Ban X, Zhang X, Hu H, Li G, Wang D, Wang CQ, Zhang F, and Shen J. 2016. MR imaging features and staging
337 of neuroendocrine carcinomas of the uterine cervix with pathological correlations. *Eur Radiol* 26:4293-
338 4302. 10.1007/s00330-016-4327-1

339 Fan C, Min X, Feng Z, Cai W, Li B, Zhang P, You H, Xie J, and Wang L. 2020. Discrimination between benign and
340 malignant testicular lesions using volumetric apparent diffusion coefficient histogram analysis. *Eur J Radiol*
341 126:108939. 10.1016/j.ejrad.2020.108939

342   Gadducci A, Carinelli S, and Aletti G. 2017. Neuroendrocrine tumors of the uterine cervix: A therapeutic challenge
343   for gynecologic oncologists. *Gynecol Oncol* 144:637-646. 10.1016/j.ygyno.2016.12.003

344   Gardner GJ, Reidy-Lagunes D, and Gehrig PA. 2011. Neuroendocrine tumors of the gynecologic tract: A Society of
345   Gynecologic Oncology (SGO) clinical document. *Gynecol Oncol* 122:190-198. 10.1016/j.ygyno.2011.04.011

346   Gu KW, Kim CK, Choi CH, Yoon YC, and Park W. 2019. Prognostic value of ADC quantification for clinical outcome in
347   uterine cervical cancer treated with concurrent chemoradiotherapy. *Eur Radiol* 29:6236-6244.
348   10.1007/s00330-019-06204-w

349   Heo SH, Shin SS, Kim JW, Lim HS, Jeong YY, Kang WD, Kim SM, and Kang HK. 2013. Pre-treatment diffusion-
350   weighted MR imaging for predicting tumor recurrence in uterine cervical cancer treated with concurrent
351   chemoradiation: value of histogram analysis of apparent diffusion coefficients. *Korean J Radiol* 14:616-625.
352   10.3348/kjr.2013.14.4.616

353   Lee J, Kim CK, and Park SY. 2020. Histogram analysis of apparent diffusion coefficients for predicting pelvic lymph
354   node metastasis in patients with uterine cervical cancer. *MAGMA* 33:283-292. 10.1007/s10334-019-
355   00777-9

356   Li J, Ouyang Y, Tao Y, Wang L, Li M, Gao L, and Cao X. 2020. Small cell carcinoma of the uterine cervix: a multi-
357   institutional experience. *Int J Gynecol Cancer* 30:174-180. 10.1136/ijgc-2019-000612

358   Liang HY, Huang YQ, Yang ZX, Ying D, Zeng MS, and Rao SX. 2016. Potential of MR histogram analyses for prediction
359   of response to chemotherapy in patients with colorectal hepatic metastases. *Eur Radiol* 26:2009-2018.
360   10.1007/s00330-015-4043-2

361   Lin G, Ho KC, Wang JJ, Ng KK, Wai YY, Chen YT, Chang CJ, Ng SH, Lai CH, and Yen TC. 2008. Detection of lymph node
362   metastasis in cervical and uterine cancers by diffusion-weighted magnetic resonance imaging at 3T. *J*
363   *Magn Reson Imaging* 28:128-135. 10.1002/jmri.21412

364   Lin LM, Lin Q, Liu J, Chu KX, Huang YX, Zhang ZK, Li T, Dai YQ, and Li JL. 2020. Prognostic factors and treatment
365   comparison in small cell neuroendocrine carcinoma of the uterine cervix based on population analyses.
366   *Cancer Med* 9:6524-6532. 10.1002/cam4.3326

367   Liu S, Guan W, Wang H, Pan L, Zhou Z, Yu H, Liu T, Yang X, He J, and Zhou Z. 2014. Apparent diffusion coefficient
368   value of gastric cancer by diffusion-weighted imaging: correlations with the histological differentiation
369   and Lauren classification. *Eur J Radiol* 83:2122-2128. 10.1016/j.ejrad.2014.09.021

370   McCann GA, Boutsicaris CE, Preston MM, Backes FJ, Eisenhauer EL, Fowler JM, Cohn DE, Copeland LJ, Salani R, and
371   O'Malley DM. 2013. Neuroendocrine carcinoma of the uterine cervix: the role of multimodality therapy in
372   early-stage disease. *Gynecol Oncol* 129:135-139. 10.1016/j.ygyno.2013.01.014

373   Meyer HJ, Gundermann P, Hohn AK, Hamerla G, and Surov A. 2019. Associations between whole tumor histogram
374   analysis parameters derived from ADC maps and expression of EGFR, VEGF, Hif 1-alpha, Her-2 and Histone
375   3 in uterine cervical cancer. *Magn Reson Imaging* 57:68-74. 10.1016/j.mri.2018.10.016

376   Nakamura K, Joja I, Nagasaka T, Fukushima C, Kusumoto T, Seki N, Hongo A, Kodama J, and Hiramatsu Y. 2012. The
377   mean apparent diffusion coefficient value (ADCmean) on primary cervical cancer is a predictive marker for
378   disease recurrence. *Gynecol Oncol* 127:478-483. 10.1016/j.ygyno.2012.07.123

379   Park JJ, Kim CK, Park SY, Park BK, and Kim B. 2014. Value of diffusion-weighted imaging in predicting parametrial
380   invasion in stage IA2-IIA cervical cancer. *Eur Radiol* 24:1081-1088. 10.1007/s00330-014-3109-x

381   Perucho JAU, Wang M, Tse KY, Ip PPC, Siu SWK, Ngan HYS, Khong PL, and Lee EYP. 2020. Association between MRI
382   histogram features and treatment response in locally advanced cervical cancer treated by

383   chemoradiotherapy. *Eur Radiol*. 10.1007/s00330-020-07217-6

384   Sala E, Wakely S, Senior E, and Lomas D. 2007. MRI of malignant neoplasms of the uterine corpus and cervix. *AJR*
385   *Am J Roentgenol* 188:1577-1587. 10.2214/AJR.06.1196

386   Satoh T, Takei Y, Treilleux I, Devouassoux-Shisheboran M, Ledermann J, Viswanathan AN, Mahner S, Provencher
387   DM, Mileshkin L, Avall-Lundqvist E, Pautier P, Reed NS, and Fujiwara K. 2014. Gynecologic Cancer
388   InterGroup (GCIG) consensus review for small cell carcinoma of the cervix. *Int J Gynecol Cancer* 24:S102-
389   108. 10.1097/IGC.0000000000000262

390   Schob S, Meyer HJ, Dieckow J, Pervinder B, Pazaitis N, Hohn AK, Garnov N, Horvath-Rizea D, Hoffmann KT, and
391   Surov A. 2017a. Histogram Analysis of Diffusion Weighted Imaging at 3T is Useful for Prediction of
392   Lymphatic Metastatic Spread, Proliferative Activity, and Cellularity in Thyroid Cancer. *Int J Mol Sci* 18.
393   10.3390/ijms18040821

394   Schob S, Meyer HJ, Pazaitis N, Schramm D, Bremicker K, Exner M, Hohn AK, Garnov N, and Surov A. 2017b. ADC
395   Histogram Analysis of Cervical Cancer Aids Detecting Lymphatic Metastases-a Preliminary Study. *Mol*
396   *Imaging Biol* 19:953-962. 10.1007/s11307-017-1073-y

397   Shaghaghi M, Aliyari Ghasabeh M, Ameli S, Ghadimi M, Hazhirkarzar B, Rezvani Habibabadi R, Khoshpouri P,
398   Pandey A, Pandey P, and Kamel IR. 2020. Post-TACE changes in ADC histogram predict overall and
399   transplant-free survival in patients with well-defined HCC: a retrospective cohort with up to 10 years
400   follow-up. *Eur Radiol*. 10.1007/s00330-020-07237-2

401   Woo S, Moon MH, Cho JY, Kim SH, and Kim SY. 2019. Diagnostic Performance of MRI for Assessing Parametrial
402   Invasion in Cervical Cancer: A Head-to-Head Comparison between Oblique and True Axial T2-Weighted
403   Images. *Korean J Radiol* 20:378-384. 10.3348/kjr.2018.0248

404   Yuan L, Jiang H, Lu Y, Guo SW, and Liu X. 2015. Prognostic Factors of Surgically Treated Early-Stage Small Cell
405   Neuroendocrine Carcinoma of the Cervix. *Int J Gynecol Cancer* 25:1315-1321.
406   10.1097/IGC.0000000000000496

407   Zhao B, Cao K, Li XT, Zhu HT, and Sun YS. 2019. Whole lesion histogram analysis of apparent diffusion coefficients
408   on MRI predicts disease-free survival in locally advanced squamous cell cervical cancer after radical
409   chemo-radiotherapy. *BMC Cancer* 19:1115. 10.1186/s12885-019-6344-3

410   Zou X, Luo Y, Li Z, Hu Y, Li H, Tang H, Shen Y, Hu D, and Kamel IR. 2019. Volumetric Apparent Diffusion Coefficient
411   Histogram Analysis in Differentiating Intrahepatic Mass-Forming Cholangiocarcinoma From Hepatocellular
412   Carcinoma. *J Magn Reson Imaging* 49:975-983. 10.1002/jmri.26253

413

414

415

416

Patient characteristics (N=83).

Abbreviations: FIGO, International Federation of Gynecology and Obstetrics; Adjuvant therapy includes chemotherapy, radiotherapy and concurrent chemoradiation; CT, chemotherapy; CCRT, concurrent chemoradiation; NACT, neoadjuvant chemotherapy.

1   Table 1. Patient characteristics (N=83).

Variables	Number(%)
Hystological type	
Small cell neuroendocrine carcinoma	80(96.4%)
Large cell neuroendocrine carcinoma	3(3.6%)
Histological homology	
Pure	57(68.7%)
Mix with squamous	7(8.4%)
Mix with adenocarcinoma	16(19.3%)
Mix with adenosquamous carcinoma	3(3.6%)
FIGO stage(2018)	
I	
IB2	6(7.2%)
IB3	3(3.6%)
II	
IIA1	13(15.7%)
IIA2	13(15.7%)
IIB	16(19.3%)
III	
IIIA	3(3.6%)
IIIC1	15(18.1%)
IIIC2	5(6.0%)
IV	
IVB	9(10.8%)
Lymph node metastasis	
Pelvic only	19(22.9%)
Pelvic and para-aortic	8(9.6%)
Negative	56(67.5%)
Primary treatment	
Surgery + adjuvant therapy	12(14.5%)
NACT + surgery ± adjuvant therapy	31(37.3%)
Surgery alone	2(2.4%)
CCRT + CT	30(36.1%)
CT alone	8(9.6%)
Chemotherapy regimen	
EP	38(45.8%)
TP	34(41.0%)
Other regimens	8(9.6%)
Without chemotherapy	3(3.6%)
Age,years(mean ± SD)	49.2±10.5
Tumor size,cm(mean ± SD)	4.7±1.9

$ADC_{mean}(10^{-3}mm^2/s,mean \pm SD)$	0.750 ± 0.293
$ADC_{max}(10^{-3}mm^2/s,mean \pm SD)$	0.969 ± 0.284
$ADC_{min}(10^{-3}mm^2/s,mean \pm SD)$	0.632 ± 0.293

ADC values and clinicopathological parameters

Abbreviations: *P values were dervied applying the Mann-Whitney U test□other P values were dervied applying the Student's t test.

1 Table 2. ADC values and clinicopathological parameters.

Variable	N	ADCmean(10^{-3}mm^2/s)	P	ADCmax(10^{-3}mm^2/s)	P	ADCmin(10^{-3}mm^2/s)	P
FIGO stage			0.001*		0.010*		0.001*
I-IIA	35	0.880 ± 0.327		1.068 ± 0.299		0.761 ± 0.345	
IIB-IVB	48	0.655 ± 0.226		0.896 ± 0.252		0.538 ± 0.206	
Age,years			0.630		0.380		0.628
≦45	30	0.729 ± 0.308		0.932 ± 0.306		0.612 ± 0.303	
> 45	53	0.762 ± 0.287		0.989 ± 0.272		0.642 ± 0.290	
Tumor size(cm)			0.002*		0.022*		0.007*
< 4	24	0.882 ± 0.305		1.069 ± 0.269		0.751 ± 0.335	
≧4	59	0.696 ± 0.274		0.928 ± 0.282		0.583 ± 0.262	
Pelvic LN metastasis			0.040		0.130		0.009
No	56	0.788 ± 0.332		1.002 ± 0.304		0.678 ± 0.329	
Yes	27	0.672 ± 0.172		0.901 ± 0.228		0.534 ± 0.165	
Para-aortic LN metastasis			0.408		0.193		0.346
Negative	75	0.759 ± 0.304		0.982 ± 0.292		0.642 ± 0.304	
Positive	8	0.668 ± 0.148		0.844 ± 0.165		0.538 ± 0.131	
Lymphovascular invasion			0.067		0.064		0.074
Negative	25	0.914 ± 0.347		1.108 ± 0.327		0.799 ± 0.345	
Positive	20	0.735 ± 0.278		0.934 ± 0.273		0.619 ± 0.301	
Depth of stromal invasion			0.040		0.023		0.055
Inner third	17	0.975 ± 0.378		1.162 ± 0.352		0.852 ± 0.380	
Middle to outer third	28	0.748 ± 0.264		0.951 ± 0.264		0.638 ± 0.281	
Histological homology			0.773		0.719		0.407
Pure	57	0.744 ± 0.288		0.961 ± 0.296		0.614 ± 0.294	
Mixed	26	0.764 ± 0.310		0.985 ± 0.263		0.671 ± 0.292	

Comparison of MRI staging and pathological staging in surgically treated patients without neoadjuvant treatment.

1 Table 3. Comparison of MRI staging and pathological staging in surgically treated patients
2 without neoadjuvant treatment.

Parameter	MRI	Pathology		Sensitivity	Specificity	Accuracy
		Positive	Negative			
Uterine corpus invasion	Positive	0	2	-	86.7%	86.7%
	Negative	0	13			
Parametrial invasion	Positive	0	3	-	80.0%	80.0%
	Negative	0	12			
Vaginal invasion	Positive	1	7	100.0%	50.0%	53.3%
	Negative	0	7			
Lymph node metastasis	Positive	1	0	50.0%	100.0%	93.3%
	Negative	1	13			

Univariate and multivariate analysis of clinicopathological and treatment parameters for the all series (n=83).

Abbreviations: SCNEC, Small cell neuroendocrine carcinoma; LCNEC, large cell neuroendocrine carcinoma;Adjuvant therapy includes chemotherapy, radiotherapy and concurrent chemoradiation; CT, chemotherapy; CCRT, concurrent chemoradiation; NACT, neoadjuvant chemotherapy; EP, etoposide and cisplatin/carboplatin; TP, paclitaxel and cisplatin/carboplatin.

1 Table 4.Univariate and multivariate analysis of clinicopathological and treatment parameters for
2 the all series (n=83).

Variable	n	Overall survival						Progression free survival					
		Univariate			Multivariate			Univariate			Multivariate		
		HR	95%CI	P	HR	95%CI	P	HR	95%CI	P	HR	95%CI	P
Hystological type		1.537	0.369-6.406	0.555				1.424	0.344-5.893	0.626			
SCNEC	80												
LCNEC	3												
Age,years		2.552	1.236-5.270	0.011	2.651	1.257-5.590	0.01	2.117	1.106-4.054	0.024	2.380	1.222-4.635	0.011
≤45	30												
>45	53												
Tumor size(cm)		2.225	1.061-6.047	0.036	1.354	0.539-3.403	0.519	1.639	0.811-3.311	0.169			
<4	24												
≥4	59												
FIGO stage(2018)		2.339	1.578-3.469	0.001	2.085	1.351-3.217	0.001	2.423	1.634-3.342	<0.001	1.919	1.221-3.014	0.005
I	9												
II	42												
III	23												
IV	9												
Histological homology		1.198	0.666-2.534	0.443				1.425	0.772-2.629	0.357			
Pure	57												
Mixed	26												
Pelvic LN metastasis		2.557	1.477-5.316	0.002	1.138	0.440-2.946	0.789	3.405	1.872-6.191	<0.001	1.576	0.615-4.036	0.343
No	56												
Yes	27												
Para-aortic LN metastasis		3.287	1.573-8.203	0.002	1.265	0.439-3.649	0.663	5.241	2.405-11.422	<0.001	3.151	1.204-8.248	0.019
No	75												
Yes	8												
Chemotherapy regimen		1.079	0.717-1.767	0.608				1.075	0.713-1.622	0.73			
TP	34												
EP	38												
Other regimens	8												
Without chemotherapy	3												
Cycle of chemotherapy		0.556	0.286-1.084	0.085	0.546	0.278-1.071	0.078	0.771	0.424-1.401	0.394			
0-5	48												
≥6	35												
ADCmin(10^{-3}mm²/s)		3.250	1.269-8.323	0.014	1.286	0.368-4.498	0.694	3.147	1.328-7.458	0.009	3.787	1.469-9.765	0.006
<0.680	61												
≥0.680	22												
ADCmax(10^{-3}mm²/s)		4.174	1.632-10.68	0.003	1.853	0.622-5.526	0.268	3.047	1.418-6.547	0.004	1.464	0.627-3.423	0.379
≤1.032	53												

>1.032	30												
ADCmean($10^{-3}mm^2/s$)		2.646	1.339-5.230	0.005	2.344	1.155-4.756	0.018	2.140	1.161-3.944	0.015	1.243	0.572-2.699	0.583
≤0.700	42												
>0.700	41												

Univariate and multivariate analysis of clinicopathological and treatment parameters for surgically treated patients (n=45).

Abbreviations: SCNEC, Small cell neuroendocrine carcinoma; LCNEC, large cell neuroendocrine carcinoma; Adjuvant therapy includes chemotherapy, radiotherapy and concurrent chemoradiation; CT, chemotherapy; CCRT, concurrent chemoradiation; NACT, neoadjuvant chemotherapy; EP, etoposide and cisplatin/carboplatin; TP, paclitaxel and cisplatin/carboplatin.

1 Table 5. Univariate and multivariate analysis of clinicopathological and treatment parameters for
2 surgically treated patients (n=45).

Variable	n	Overall survival						Progression free survival					
		Univariate			Multivariate			Univariate			Multivariate		
		HR	95%CI	P	HR	95%CI	P	HR	95%CI	P	HR	95%CI	P
Hystological type		1.194	0.157-9.104	0.864				0.960	0.128-7.202	0.968			
SCNEC	43												
LCNEC	2												
Age,years		1.458	0.538-3.944	0.459				1.358	0.559-3.301	0.499			
≦45	21												
＞45	24												
Tumor size(cm)		2.193	0.707-6.807	0.174				1.339	0.534-3.361	0.534			
＜4	19												
≧4	26												
FIGO stage(2018)		2.623	1.094-6.288	0.031	0.882	0.309-2.516	0.815	2.673	1.221-5.852	0.014	0.716	0.129-3.964	0.702
I	8												
II	28												
III	9												
Histological homology		1.435	0.534-3.851	0.474				1.821	0.750-4.420	0.185			
Pure	24												
Mixed	21												
Pelvic LN metastasis		2.165	0.744-6.299	0.156				2.653	1.049-6.713	0.039	1.706	0.622-4.683	0.300
No	35												
Yes	10												
Lymphovascular invasion		4.207	1.441-12.285	0.009	3.241	1.105-9.505	0.032	3.055	1.211-7-708	0.018	1.562	0.556-4.392	0.398
Negative	25												
Positive	20												
Depth of stromal invasion		4.203	1.173-15.056	0.027	2.36	0.598-9.320	0.220	3.520	1.152-10.754	0.027	2.639	0.846-8.230	0.095
Inner third	17												
Middle to outer third	28												
Neoadjuvant therapy		1.171	0.403-3.399	0.771				1.032	0.394-2.700	0.949			
No	15												
Yes	30												
Chemotherapy regimen		0.782	0.352-1.740	0.547				0.929	0.473-1.825	0.831			
TP	17												
EP	20												
Other regimens	6												
Cycle of chemotherapy		0.48	0.173-1.334	0.159				0.747	0.293-1.903	0.54			
0-5	21												
≧6	24												

Variable	n												
ADCmin(10⁻³mm²/s)		11.49	1.515-87.163	0.018	1.440	0.096-21.552	0.792	6.983	1.616-30.173	0.009	2.084	0.287-15.12	0.468
<0.680	28												
≧0.680	17												
ADCmax(10⁻³mm²/s)		16.69	2.230-128.977	0.006	14.413	1.883-110.342	0.01	6.667	1.945-22.850	0.003	5.668	1.634-19.66	0.006
≦1.032	24												
>1.032	21												
ADCmean(10⁻³mm²/s)		4.194	1.447-12.160	0.008	1.257	0.345-4.578	0.729	2.740	1.118-6.717	0.028	3.655	0.639-20.91	0.145
≦0.700	18												
>0.700	27												

Figure 1

A 45-year-old female patient with NECC.

A: Sagittal T2-weighted image. B: Axial T1-enhanced image. C. DWI in b=800. D:ADC map.
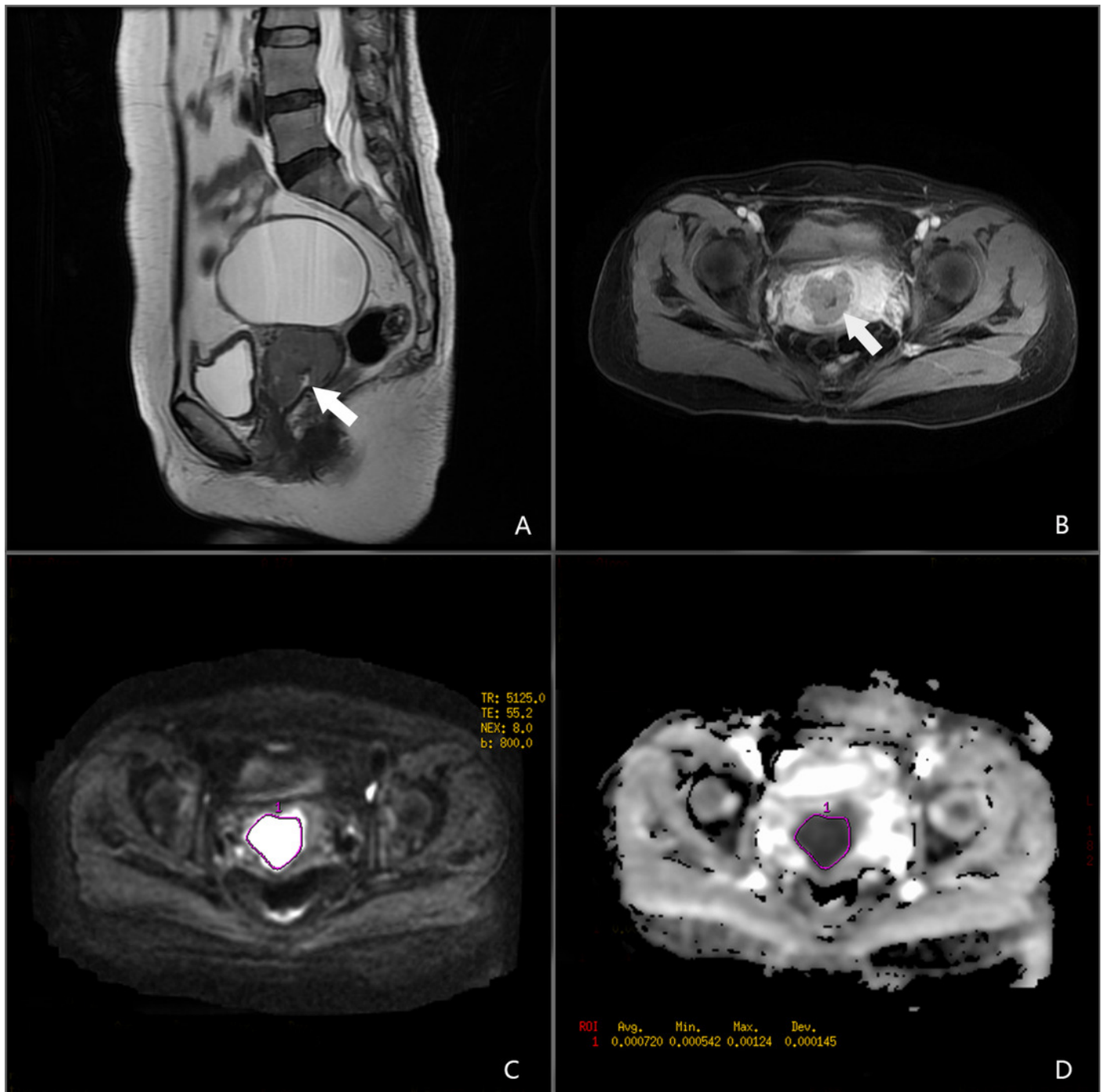
Figure 2

ROC curves of ADC_{max}, ADC_{mean}, ADC_{min} for OS and PFS.

A ROC curve of ADCmax for OS

AUC=0.717
(95%CI 0.605–0.830)
P<0.001

B ROC curve of ADCmax for PFS

AUC=0.696
(95%CI 0.577–0.814)
P=0.002

C ROC curve of ADCmean for OS

AUC=0.680
(95%CI 0.565–0.796)
P=0.005

D ROC curve of ADCmean for PFS

AUC=0.664
(95%CI 0.542–0.785)
P=0.011

E ROC curve of ADCmin for OS

AUC=0.614
(95%CI 0.492–0.736)
P=0.074

F ROC curve of ADCmin for PFS

AUC=0.633
(95%CI 0.507–0.758)
P=0.038
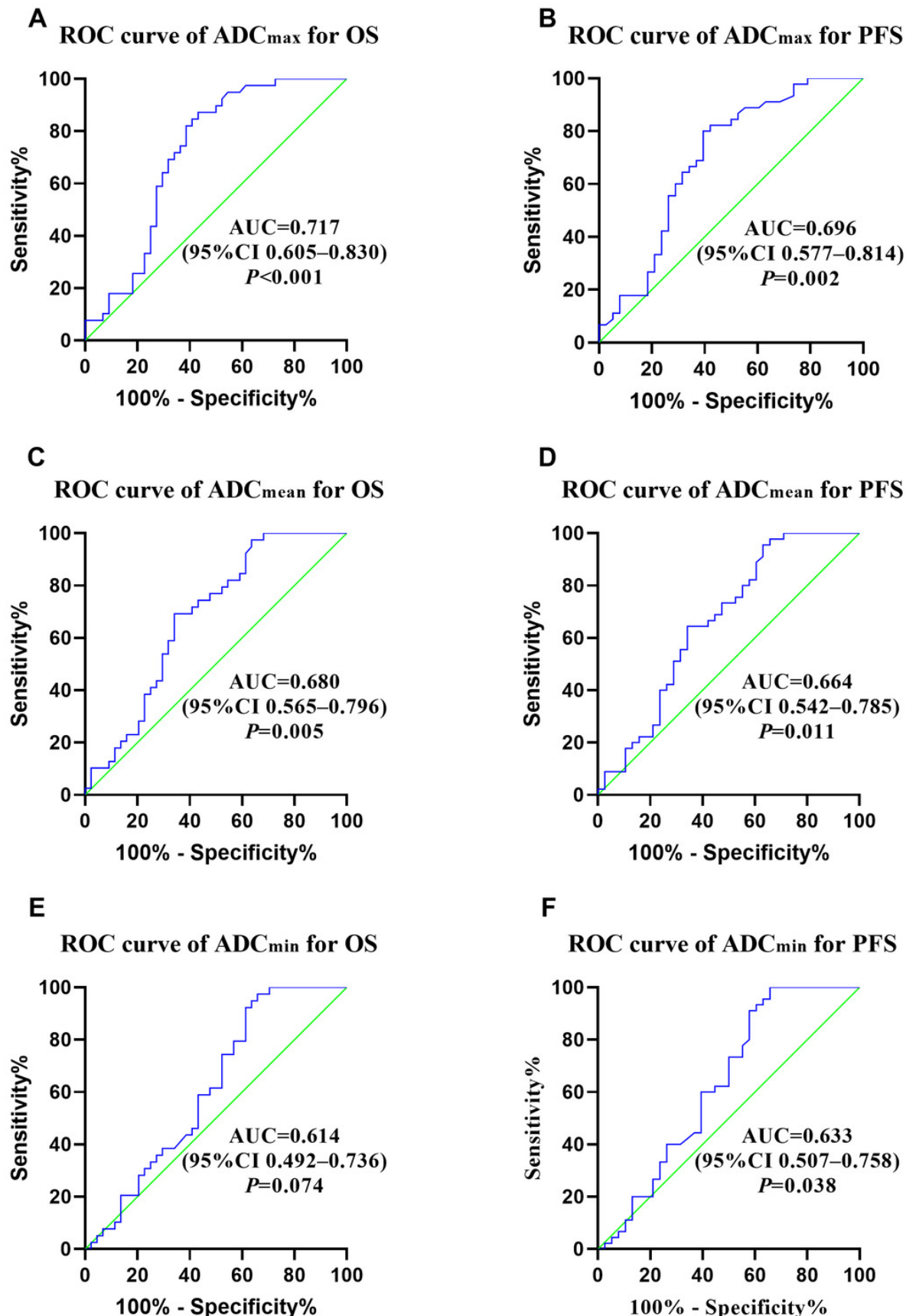
Figure 3

Survival curves of different ADC vaules.

(A), (C) and (E) for OS, (B), (D) and (F) for PFS.
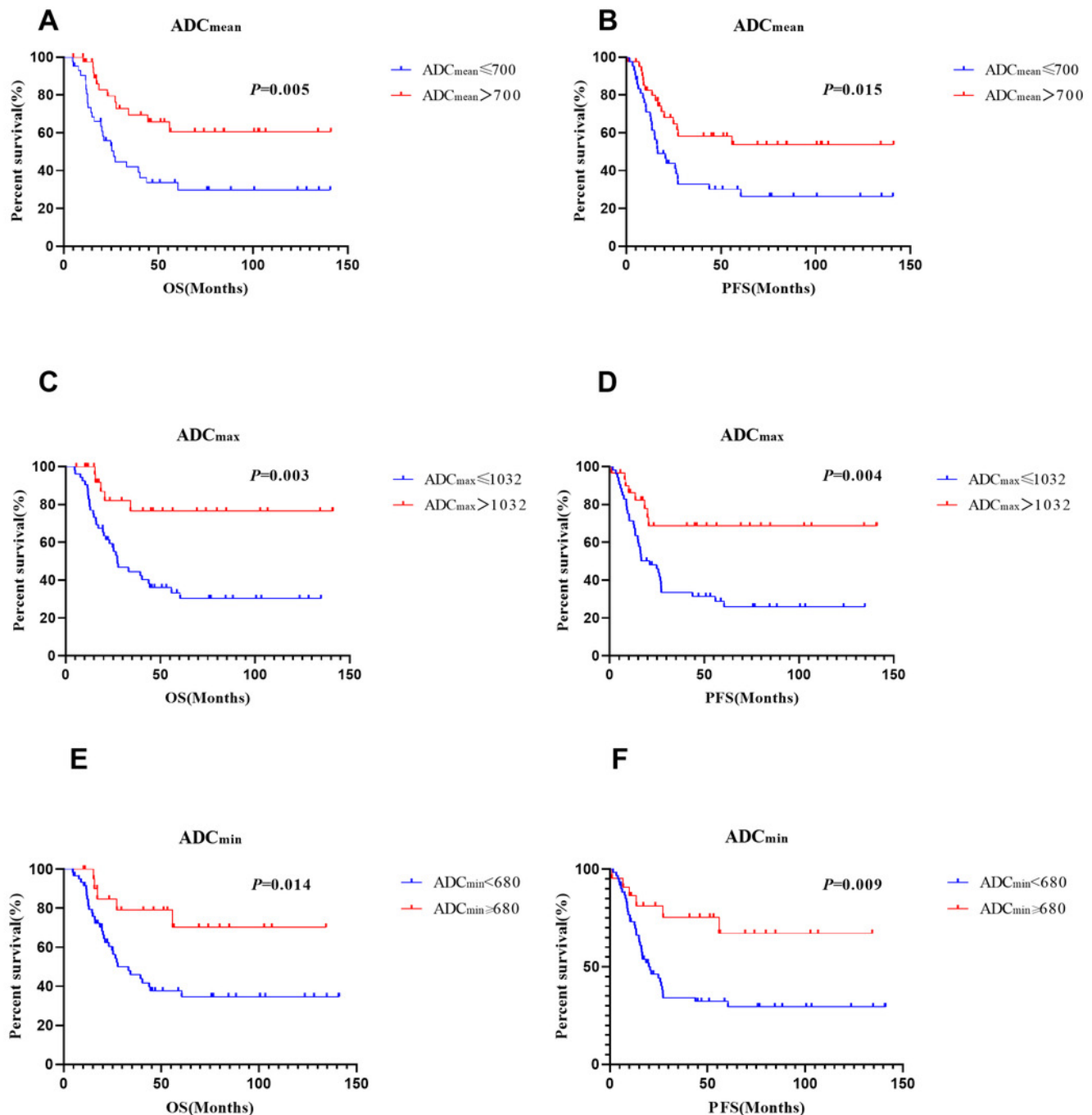
Figure 4

Survival curves of different FIGO stage, age and para-aortic lymph nodestatus.

(A), (C) and (E) for OS, (B), (D) and (F) for PFS.